Desalination and Water Treatment
www.deswater.com

doi: 10.5004/dwt.2018.22528

121 (2018) 327–331
July

UWB wireless connection for building water supply leakage monitoring system

Runfeng Yang[a,*], Jian Zhao[b], Xiaoning Chen[a]

[a]*Department of Electronic Engineering, Dongguan Polytechnic, Dongguan, China, emails: yangrf@dgpt.edu.cn (R. Yang), chenxn@dgpt.edu.cn (X. Chen)*
[b]*School of Information and Technology, Northwest University, Xi an, China, email: zjctec@nwu.edu.cn (J. Zhao)*

Received 23 February 2018; Accepted 21 May 2018

ABSTRACT

Water leakage monitoring and throttling device are provided utility with a smart detecting solution to prevent leakage for the water supply and drainage in smart building. Ultra wideband (UWB) technology is one of the Internet of things (IoT) solutions to connect water monitoring and throttling devices in smart building based on bidirectional high speed communication. This paper presents a study of UWB propagation channel, system model, and system testing configuration in multipath performance of indoor simulation model. Theoretical analysis and experimental results demonstrate different measured system performance from 200 to 480 Mb/s, which has the capability to flow the data between devices in a smart building.

Keywords: UWB; Smart building; Leakage monitoring

1. Introduction

In smart building, water leakage monitoring and throttling device are used as a smart detecting solution to prevent leakage for the water supply and drainage, which improve environmental efficiencies and higher returns by optimizing the use of water and reduce energy consumption and costs. A water alert will be sent from a water detection sensor in which a leak has been detected so that the problem can be addressed as quickly as possible. Hence, the reliable communication speed and coverage are important to the system. Ultra wideband (UWB) technology is widely used in the Internet of things (IoT) for extending the wireless link coverage. The water monitoring and throttling devices in smart building can connect IoT based on UWB with bi-directional high-speed communication.

The networking of things such as sensors and actuators is the basic enabler for machine-to-machine/man connectivity. Things can be connected using wired or wireless technologies depending on the home environment. For a wireless connection, short-range and long-range radio links provide two different communication paradigms to fit for different system architectures. Wireless sensor network (WSN) protocols have enabled WSNs to dominate the M2M connectivity technology in smart buildings. A combination of short-range WSNs and the cellular network is sometimes referred as a capillary network which enjoys a complete wireless connectivity for home devices using a cellular-connected gateway to exchange WSNs data to the Internet through cellular radio [1]. Perumal et al. [2] defined three interoperability levels for heterogeneous systems. Hwang [3] pointed out that the simple self-configuration and self-healing mechanism provided by Zigbee specification is too slow. Bluetooth Special Interest Group (SIG) has recently setup the Bluetooth Smart Mesh Working Group to promote the technology for IoT.

UWB specification has been defined as a high-speed wireless connectivity targeting at 480 Mb/s with low power targeting at 100 mW for a distance about 3 m over severe multipath, but a lower data rate operation can be remained with extended distances at about 10 m. In UWB radio transmission,

* Corresponding author.

Presented at the 3rd International Conference on Recent Advancements in Chemical, Environmental and Energy Engineering, 15–16 February, Chennai, India, 2018

the transmitted signal using an extremely wide transmission bandwidth and low power offers potential benefits in transporting high data rates over short distance, multipath and fading immunity, low implementation cost, even communication, and accurate ranging between UWB devices at the same time. Multipath cancellation causes a reduced amplitude response for the direct path signal occurring in the receiver. With the very short UWB pulses having a width as small as one nanosecond or less, the transmitted signal from direct path is received in phase before the reflected path arrives, thus avoiding the multipath cancellation. The UWB spectrum is operated with a multiband scheme which allows the selective implementation of bands and offers the dynamic ability for regulatory problems. Furthermore, by using smaller subbands to transmit the information, the processing bandwidth for the receiver can be reduced, thus reducing the power consumption of the radio, and lowering the cost for device implementation. Orthogonal frequency division multiplexing (OFDM) is a promising solution for the design of UWB system to efficiently capture multipath energy and deliver the high data rate transmission in highly dispersive UWB channels.

2. UWB channel model

The fundamental issue of UWB is that the transmitted signal can be spread over an extremely large bandwidth with very low power spectral density (PSD). In early 2002, the USA Federal Communications Commission (FCC) agreed to allocate 7,500 MHz radio frequency spectrum in 3.1–10.6 GHz band for unlicensed use for the UWB devices and limit the UWB effective isotropic radiated power (EIRP) to –41.3 dBm/MHz. The goal of the UWB channel modeling is to develop a tool that can statistically represent the channel with a number of parameters to generate the measured channel behavior in computer simulations. The Saleh-Valenzuela (S-V) model [4,5] provided better modeling to channel characteristics from the measurement data. In order to identify typical channel characteristics in the GHz region, Pendergrass [6] providing large measurement database was created from 11 different residential and office environments complex with 369 metal stud measurements and 60 wood stud measurements. The higher complexity of the channel offering the closer statistical channel modeling will benefit accurate simulation.

The IEEE 802.15.3a standards was written from the S-V model as the fundamental model with main contributions considered from other channel models to create four standard UWB channels for testing [7]. Channel Model 1 (CM1) is a line of sight multipath propagation channel of 0–4 m in length. Channel Model 2 (CM2) is a non-line of sight multipath propagation channel of 0–4 m in length. Channel Model 3 (CM3) is a non-line of sight multipath propagation channel of 4–10 m in length. Channel Model 4 (CM4) is an extreme non-line of sight multipath propagation channel of 4–10 m in length. A lognormal distribution was used for the measurement data. Independent fading is assumed for each cluster and each ray within the cluster. The discrete time impulse response of the multipath model is described as the following:

$$h_i(t) = X_i \sum_{l=0}^{L} \sum_{k=0}^{K} \alpha_{k,l}^{i} \delta(t - T_l^i - \tau_{k,l}^i) \tag{1}$$

where i refers to the impulse response realization, l refers to the cluster, k refers to the arrival within the cluster, X_i is the lognormal shadowing for the ith channel realization, $\alpha_{k,l}^{i}$ are the multipath gain coefficients, T_l^i is the delay of the lth cluster for the ith channel realization, and $\tau_{k,l}^i$ is the delay of the kth path within the lth cluster relative to the first path arrival time T_l for the ith channel realization.

The channel coefficients $\alpha_{k,l}^{i}$ are defined as the following:

$$\alpha_{k,l} = p_{k,l} \xi_l \beta_{k,l} \tag{2}$$

$$20\log 10(\xi_l \beta_{k,l}) \propto \text{Normal}(\mu_{k,l}, \sigma_c^2 + \sigma_r^2) \tag{3}$$

$$\left|\xi_l \beta_{k,l}\right| = 10^{(\mu_{k,l} + n_c + n_r)/20} \tag{4}$$

where $p_{k,l}$ is either +1 or –1 to account for signal inversion due to reflections. ξ_l reflects the fading associated with the lth cluster, and $\beta_{k,l}$ corresponds to the fading associated with the kth ray of the lth cluster. $n_c \propto \text{Normal}(0, \sigma_c^2)$ and $n_r \propto \text{Normal}(0, \sigma_r^2)$ are independent and correspond to the fading on each cluster and ray, respectively. Normal(0,σ^2) denotes a Gaussian distribution with zero mean and variance σ^2.

And the $m_{k,l}$ (the magnitude decay due to time) is given by the following equation:

$$\mu_{k,l} = \frac{10\ln(\Omega_0) - 10T_l/\Gamma - 10\tau_{k,l}/\gamma}{\ln(10)} - \frac{(\sigma_1^2 + \sigma_2^2)\ln(10)}{20} \tag{5}$$

where Ω_0 is the mean energy of the first path of the first cluster.

By definition, $\tau_{0,l} = 0$. The distribution of cluster arrival time T_l and the ray arrival time $\tau_{k,l}$ are given by the following equation:

$$p(T_l \left| T_{l-1}\right.) = \Lambda \exp\left[-\Lambda(T_l - T_{l-1})\right], \quad l > 0 \tag{6}$$

$$p(\tau_{k,l} \left| \tau_{(k-1),l}\right.) = \lambda \exp\left[-\lambda(\tau_{k,l} - \tau_{(k-1),l})\right], \quad k > 0 \tag{7}$$

where Λ refers to cluster arrival rate and λ refers to ray arrival rate (the arrival rate of the a path within each cluster). And the shadowing term is described by the following:

$$20\log 10(X_i) \propto \text{Normal}(0, \sigma_x^2) \tag{8}$$

The averaged power delay profile reflects the exponential decay of each cluster and decay of the total cluster power with delay, as described in the following:

$$E\left[\left|\xi_l \beta_{k,l}\right|^2\right] = \Omega_0 e^{-T_l/\Gamma} e^{-\tau_{k,l}/\gamma} \tag{9}$$

Each channel has defined 100 actual realizations with the same means and standard deviations of lognormal

shadowing. However, every channel has different arrival rates and decay factors. The multipath channel characteristics and model parameters can be found in Table 1. It is also assumed that devices will be stationary and therefore the channels are time invariant exhibiting no Doppler effect during the transmission period of each packet. Channel modeling profiles for all the variety of channel realizations in each of the four channels are given as MATLAB data files (.mat) system computation, which provide different powers, times, and impulse responses for accurate simulation of UWB propagation channels.

3. System model

To operate the physical layer (PHY) service interface to the medium access control (MAC) service, a physical layer convergence protocol (PLCP) sublayer is defined to provide a method for converting a PHY service data unit (PSDU) into a PLCP packet data unit composed from three components (shown in Fig. 1): the PLCP preamble, the PLCP header, and the PSDU. The PLCP preamble contains of two portions: a packet/frame synchronization sequence aimed at packet acquisition and detection, coarse carrier frequency estimation, coarse symbol timing, and synchronization within the preamble; and a channel estimation (CE) sequence aiming at frequency response estimation, fine carrier frequency estimation, and fine symbol timing. Reed–Solomon code is employed in order to improve decoding at the receiver offering good reliability performance in the mobile environment [8]. Each OFDM symbol is constructed from the inverse fast Fourier transform (IFFT) of a set of 128 complex valued carriers made from 100 data carriers, 12 pilot carriers, 6 NULL valued carriers, and 10 guard carriers. The 10 guard carriers used for mitigating intersymbol interference are located on either edge of the OFDM symbol and they are the same value as the 5 outermost data carries. In addition, the guard carriers are considered as another form of time and frequency diversity resulting in improved performance for the receiver. The transmitter may reduce the power on the guard pilot carriers with the objective to relax the specifications of the transmit filters.

MAC header and header check sequence, and the entire PSDU are scrambled with a 15-bits initialization vector. The initialization vector is controlled by four different seed identifier values that are incremented in a two-bit rollover counter for each frame sent by the PHY. Convolutional coding is for error control of digital data transmission, known as a typical type of forward error correction, which allows the receiver to detect and correct errors. R = 1/3, K = 7 convolutional code is used for the convolutional encoder with generator polynomial $g_0 = 133_8$, $g_1 = 165_8$, and $g_2 = 171_8$, where $[.]_8$ refers to the octal representation of the polynomial. A puncturer is used to remove some of the encoded bits at the transmitter, which can reduce the number of transmitted bits to achieve different coding rates without significantly increasing the system complexity. The PLCP header is encoded only using a coding rate of R = 1/3. The PSDU is encoded with puncturing to achieve appropriate coding rate of R = 1/3, 1/2, 5/8, or 3/4 depending on the selected operation modes. The coded and padded bit stream is interleaved in three distinct stages. Firstly, symbol interleaver enables the PHY to exploit frequency diversity within a band group via permuting the bits across six consecutive OFDM symbols. Secondly, intra-symbol tone interleaver exploits frequency diversity across subcarriers and provides robustness against narrow-band interferes via permuting the bits across the data subcarriers within an OFDM symbol. Finally, intra-symbol cyclic shifters cyclically shift the deterministic amounts of bits in successive OFDM when the time division spreading (TDS) and fix frequency interleaving modes are enabled.

To transmit a PSDU that contains the information bits, the proposed high-speed wireless USB system offers different

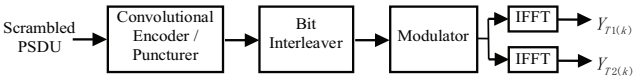

Fig. 1. Encoding process for the scrambled PSDU at transmitter.

Table 1
Multipath channel characteristics and corresponding model parameters [6]

Model parameters	CM1	CM2	CM3	CM4
Λ, cluster arrival rate (1/ns)	0.0233	0.4	0.0667	0.0667
λ, ray arrival rate (1/ns)	2.5	0.5	2.1	2.1
Γ, cluster decay factor	7.1	5.5	14.00	24.00
γ, ray decay factor	4.3	6.7	7.9	12
σ_1, standard deviation of cluster fading (dB)	3.3941	3.3941	3.3941	3.3941
σ_2, standard deviation of ray fading (dB)	3.3941	3.3941	3.3941	3.3941
σ_x, standard deviation of shadowing (dB)	3	3	3	3
Model characteristics				
Mean excess delay (ns) (τ_m)	4.9	9.4	13.8	26.8
RMS delay (nsec) (τ_{rms})	5	8	14	26
$NP_{(10dB)}$, number of significant paths within 10 dB of peak	13.3	18.2	24.9	41.4
$NP_{(85\%)}$, number of significant paths capturing > 85%	21.4	37.2	62.7	122.8
Channel energy mean (dB)	–0.5	–0.1	0.2	0.1
Channel energy standard (dB)	2.9	3.3	3.4	3.2

RMS, root mean squared; NP, number of significant paths.

transmission modes by applying various levels of coding and diversity to offer 53.3, 80, 106.7, 160, 200, 320, 400, and 480 Mb/s in single antenna system. After bit interleaving, the coded and interleaved binary data sequence is mapped onto a quadrature phase-shift keying, dual carrier modulation, dual circular 32-quadrature amplitude modulation complex constellation. The resulting complex numbers are loaded onto the data subcarriers of the OFDM symbol implemented using an IFFT to create real or complex baseband signal. Figs. 1 and 2 depict the encoding and decoding process for the scrambled PSDU, respectively. The Channel estimator outputs an inverted channel response to remove the need for a complex division and reduce the equalizer to a complex multiplier, However, care need to be taken to manage the three different actions for TDS and frequency division spreading. The symbol input to equalizer is derived from the receiver fast Fourier transform (FFT) and cyclic extension as described above. The control block manages the required actions for the three different TDS and TDS cases.

4. System performance measurements

Simulating system performance is an important criterion in order to compare with current literature. However, the literature on MB-OFDM system performance for measuring propagation with respect to distance is surprisingly sparse. We now follow the original Multiband OFDM Alliance Special Interest Group (MBOA-SIG) MB-OFDM proposal settings [9] and adopt the new assumptions from European Computer Manufacturers Association (ECMA)-386 to simulate the UWB system with the standard UWB channels.

4.1. Propagation distance measurement

The received signal power is calculated from the difference between the total transmit power and path loss. Because the FCC defines the average power as 1 mW/MHz, the total transmitted power can be obtained from the PSD and the operating bandwidth. The total transmitted power P_{TX} can be described in Eq. (10) assuming no power loss at the transmitter and 0 dBi transmit antenna gain.

$$P_{TX} = -41.25 + 10\log_{10}(f_U - f_L)\,\text{dBm} \tag{10}$$

where –41.25 dBm/MHz is the UWB EIRP/MHz, f_L = 3,168 MHz is the lower frequency of the operating bandwidth, f_U is upper frequency varying from band group 1 (BG1) to BG6. However, BG1 is targeted for the first generation UWB devices and is also a mandatory mode, thus f_U = 4,752 MHz is assigned.

The free-space propagation model is defined under IEEE 802.15.3a, which specifies the path loss attenuating the transmitted signal as a function of the lower and upper frequencies of the operating bandwidth. The path loss P_L can be expressed as the following:

$$P_L = 20\log_{10}\left(\frac{4\pi f_g d}{c}\right)\text{dB} \tag{11}$$

where f_g = 3,882 MHz is the geometric mean of the lower and upper frequencies in BG1. The geometric mean offers a more reasonable value for the expected path loss in the system [10]. d is the distance measured in meters between the transmitter and receiver. $c = 3 \times 10^8$ m/s is the speed of light.

As a result, the function of received signal power, as described in Eq. (12), can be derived from Eqs. (10) and (11) with transmitter and receiver antenna gain (G_T, G_R).

$$P_{RX} = P_{TX} + G_T + G_R - P_L\,\text{dBm} \tag{12}$$

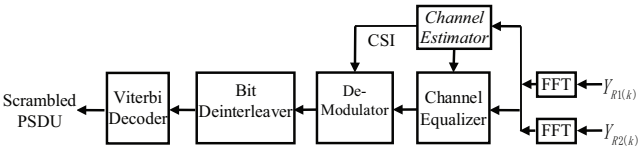

Fig. 2. Decoding process for the scrambled PSDU at receiver.

4.2. System configuration

The proposed UWB system is simulated in a realistic multipath channel environment of 100 channel realizations in the four UWB channel modeling environments CM1-CM4. The simulation results are averaged over at least 500 packets with a payload of 1,024 octet each in the PSDU and

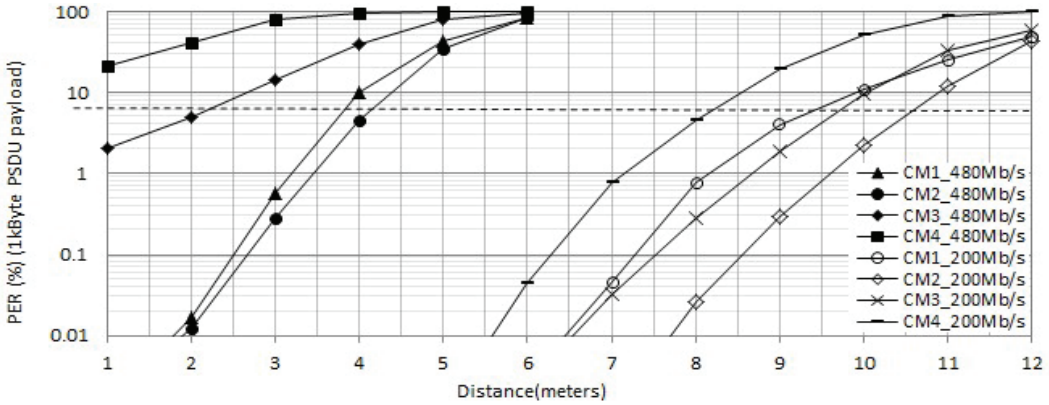

Fig. 3. System performance in CM1-CM4.

90th-percentile channel realization (the worst 10% channels are discarded). The link success probability is defined as the 90th-percentile of channel realizations for which system can successfully acquire and demodulate a packet with a packet error rate (PER) (a packet is in error if at least one bit is in error) of less than 8% [11]. PER as a function of distance, will be used as a performance indicator for the system performance measurement.

The original MBOA-SIG proposal specifies implementation loss affecting the practical system, which includes frond-end filtering, clipping at the digital-to-analog converter, analog-to-digital converter degradation, CE, clock frequency mismatch (±20 ppm at the transmitter and receiver), carrier offset recovery, carrier tracking, etc. Similarly, ECMA-368 specifies the total implementation loss of 2.5 dB and a margin of 3 dB as an assumption. It should be noted that ECMA-368 only defines the performance for reference sensitivity, not multipath. This paper will revert back to multipath test performed in the original MBOA-SIG tests when appropriate. The simulation will maintain strict adherence to timing (no frequency offset and perfect OFDM symbol timing) and use a hopping characteristic of time–frequency code = 1 and incorporate 6.6 dB noise figure referenced at the antenna and 2.5 dB implementation loss in the floating-point system model. The FFT processing in the UWB receiver requires only 6 bits externally to represent the received symbols and 12 bits of numerical precision internal to the FFT [12].

The system performance model has been simulated on the four channel models, as shown in Fig. 3. System performance on 200 Mb/s mode is between 8 and 11 m on CM1-CM4. The system for 200 Mb/s mode has been meet the WiMedia's requirements performing with extended distances of about 10 m at the lower data rates. System performance on 480 Mb/s mode is approximately 4 m on CM1 and CM2. The performances are poor when using CM3 and CM4, which means UWB system is not suitable for running high speed transmission over 4 m on non-line-of-sight multipath propagation channel. The system performance can be achieved up to 4 m at 480 Mb/s. However, it is not suitable for running high speed transmission over 4 m on non-line-of-sight multipath propagation channel. A performance gain can be achieved, while the system performance is 3.8 m in MBOA-SIG proposal, which proves UWB in high speed connectivity is extended as the targeting distance of 4 m. Because the standard has been set for the transmitter, optimization of the receiver becomes paramount to maximize the UWB system performance. The solutions of improving UWB system need to be cost-effective for implementing the low-power and high-performance device.

5. Conclusion

WiMedia Alliance working with ECMA established MB-OFDM UWB radio platform as the global UWB standard offering fast processing speed and low power requirements for IoT applications. The system was simulated in a realistic multipath channel environment of 100 channel realizations in the UWB channel environments. UWB system offers a low-cost wireless service for in smart building. It is an ideal utility for IoT solutions to connect wireless devices, and it provides a common platform for building stronger water monitoring and throttling devices applications.

Acknowledgment

The authors acknowledge Universities and Scientific Research Institutions Science and Technology Project of Dongguan City (Grant Nos.: 2016108101044, 2017507156393).

References

[1] J. Sachs, Capillary networks—a smart way to get things connected, Ericsson Rev., 8 (2014) 2–4.
[2] T. Perumal, A.R. Ramli, C.Y. Leong, S. Mansor, K. Samsudin, Interoperability Among Heterogeneous Systems in Smart Home Environment, IEEE International Conference on Signal Image Technology and Internet Based Systems, 2008, pp. 177–186.
[3] K.I. Hwang, Designing Robust ZigBee Networks with Enhanced Self-Configuration, IEEE International Conference on Consumer Electronics, 2009, pp. 1–2.
[4] A. Saleh, R. Valenzuela, A statistical model for indoor multipath propagation, IEEE J. Sel. Areas Commun., 5 (1987) 128–137.
[5] H. Hashemi, Impulse response modeling of indoor radio propagation channels, IEEE J. Sel. Areas Commun., 11 (1993) 967–978.
[6] R. Yang, R.S. Simon, Multiband OFDM Modulation and Demodulation for Ultra Wideband Communications, Novel Applications of the UWB Technologies, InTech, London, UK, 2011, pp. 1–30.
[7] P. Huang, Y. Du, Y. Li, Stability analysis and hardware resource optimization in channel emulator design, IEEE Trans. Circuits Syst. I Regul. Pap., 63 (2016) 1089–1100.
[8] P.D. Huang, A novel structure for Rayleigh channel generation with consideration of the implementation in FPGA, IEEE Trans. Circuits Syst. II Express Briefs, 63 (2016) 216–220.
[9] P. Gunturi, N. Emanetoglu, D. Kotecki, A 250-Mb/s data rate IR-UWB transmitter using current-reused technique, IEEE Trans. Microwave Theory Tech., 65 (2017) 4255–4265.
[10] R. Yang, R. S. Sherratt, Fixed Point Dual Carrier Modulation Performance for Wireless USB, IEEE International Symposium on Consumer Electronics, Kyoto, Japan, 2009, pp. 325–328.
[11] J. Kimionis, A. Collado, Octave and decade printed UWB rectifiers based on nonuniform transmission lines for energy harvesting, IEEE Trans. Microwave Theory Tech., 65 (2017) 4326–4334.
[12] A. Goavec, M. Zarudniev, An efficient method of power spectral density estimation for on-chip IR-UWB transmitter self-calibration, IEEE Trans. Circuits Syst. I Regul. Pap., 64 (2017) 686–695.